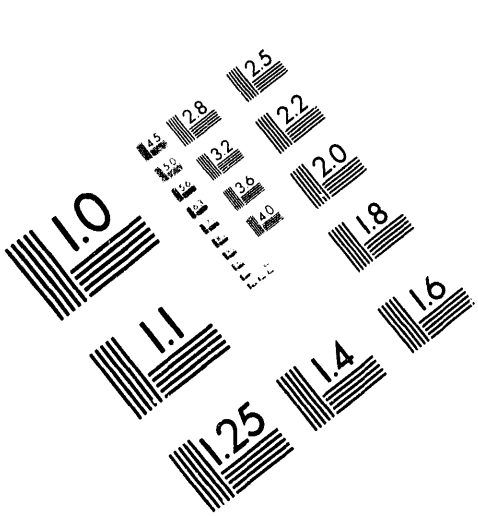

Association for Information and Image Management
1100 Wayne Avenue, Suite 1100
Silver Spring, Maryland 20910
301/587-8202

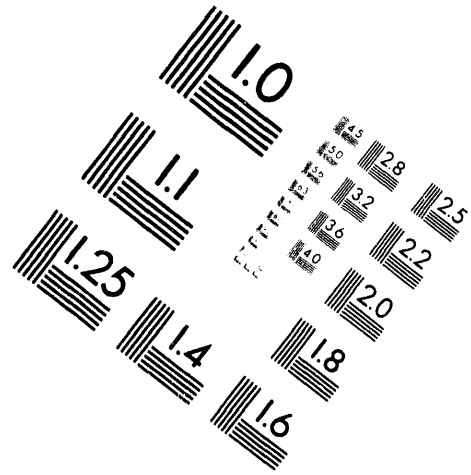

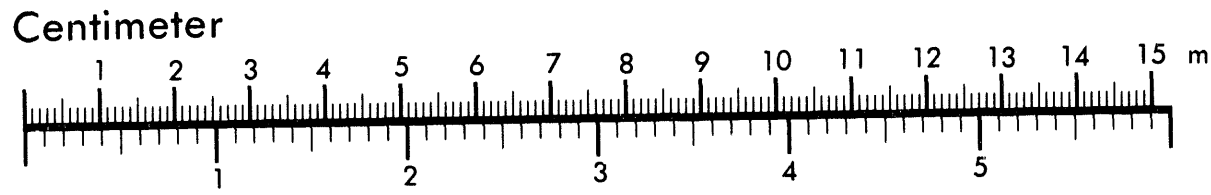

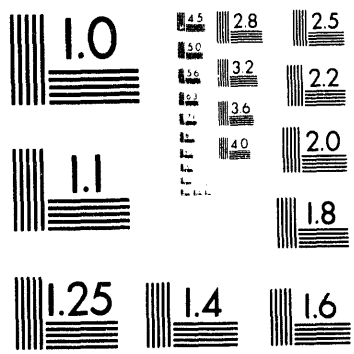

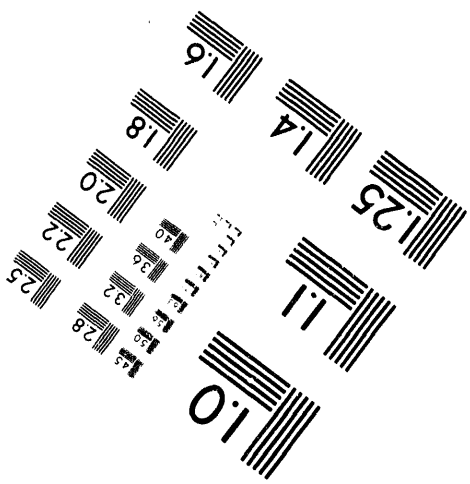

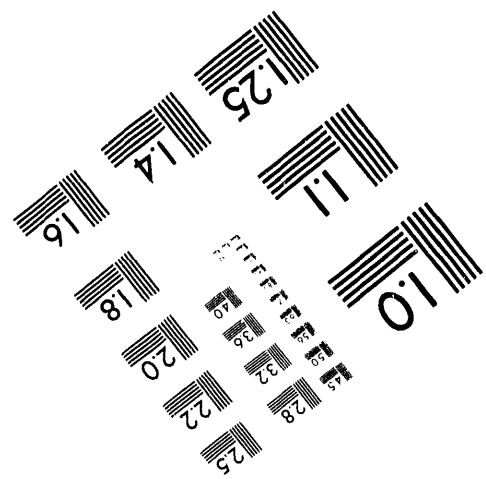

1 of 1

12

Conf-940883--6

PNL-SA-24680

ALTERNATIVE MATERIALS FOR SOLID OXIDE FUEL CELLS

J. W. Stevenson
T. R. Armstrong

August 1994

Presented at the
Fuel Cells '94 Contractor's Review Meeting
August 17-18, 1994
Morgantown, West Virginia

Prepared for
the U.S. Department of Energy
under Contract DE-AC06-76RLO 1830

Pacific Northwest Laboratory
Richland, Washington 99352

Alternative Materials For Solid Oxide Fuel Cells

CONTRACT INFORMATION

Contract Number (FTPA)	13822
Contractor	Pacific Northwest Laboratory Operated for the U.S. Department of Energy by Battelle Memorial Institute under contract DE-AC06-76RLO 1830 P.O. Box 999 Richland, Washington 99352 (509) 375-3938
Contractor Project Managers	Dr. Timothy R. Armstrong
Principle Investigators	Dr. Timothy R. Armstrong Dr. Jeffry W. Stevenson
METC Project Manager	Diane Hooie
Period of Performance	April 1, 1989 to June 30, 1994

Schedule and Milestones

FY94 Program Schedule

	S O N D J F M A M J J A S
Materials Development and Property Evaluation	----------
Materials Synthesis	
Materials Processing and Fabrication	----------
Electrochemical Processes	----------

OBJECTIVES

The purpose of this research is to develop alternative materials for solid oxide fuel cell (SOFC) interconnections and electrodes with improved electrical, thermal, and electrochemical properties. A second objective is to develop synthesis and fabrication methods for these materials whereby they can be processed in air into SOFCs. The approach is to (1) develop modifications of the current, state-of-the-art materials used in SOFCs, (2) minimize the number of cations used in the SOFC materials to reduce potential deleterious interactions, (3) improve thermal, electrical, and electrochemical properties, (4) develop methods to synthesize both state-of-the-art and alternative materials for the simultaneous fabrication and consolidation in air of the interconnections and electrodes with the solid electrolyte, and (5) understand electrochemical reactions at materials interfaces and the effects of component composition and processing on those reactions.

BACKGROUND INFORMATION

Solid oxide fuel cells (SOFCs) continue to

develop as promising, clean, and efficient technology for the direct conversion of hydrogen and fossil fuels to electrical energy. The standard materials utilized in state-of-the-art designs are: the air electrode, La(Sr)MnO_3; the fuel electrode, ZrO_2•Ni cermet; the interconnection, La(Mg)CrO_3 or La(Sr)CrO_3; and the electrolyte, Y_2O_3-stabilized ZrO_2. The required combination of these different materials in state-of-the-art SOFCs poses several materials fabrication and performance related problems.

New alternative materials with improved properties that can be more easily fabricated into fuel cells are needed for the further development of cost efficient and improved performance SOFCs. An important key is the development of a SOFC interconnection material that can be sintered in air to a high density at temperatures less than 1500°C. It should have a good thermal expansion match with, and intimately bond to, both the air and fuel electrodes, without deleterious interactions at the interfaces. At the present time this goal has not been attained with the state-of-the-art $La_{1-x}Sr_xCrO_3$ interconnections.

PROJECT DESCRIPTION

The overall approach for this research and development is to:

- Minimize the number of cations in the electrode, electrolyte, and interconnection by developing yttrium compounds, such as Y(Ca)CrO_3 as the interconnection, and Y(M')MnO_3 as the air electrode.

- Develop advanced synthesis and fabrication processes for air sintering, below 1500°C, of chromite interconnections through (1) the use of sintering aids; and (2) the synthesis of sub-micrometer powders.

- Establish methods for the simultaneous processing and consolidation of air-sinterable powders.

- Electrochemically evaluate interface reactions (in reproducible and controlled laboratory tests) for both the alternate and state-of-the-art materials and cell components developed under this program.

- Evaluate the chemical reactivity and interdiffusion effects that take place between the various fuel cell components: electrolyte/cathode, interconnect/cathode, and interconnect/anode.

This paper summarizes a comprehensive study that assessed the effect of ambient oxygen partial pressure on the stability of air-sinterable chromites and the sintering behavior of doped lanthanum manganites.

RESULTS

Stability of Chromite Interconnects

The interconnect in a solid oxide fuel cell must be electrically conducting and simultaneously stable in both oxidizing and reducing environments at high temperature. These extreme conditions restrict the viable candidate materials to lanthanum or yttrium chromites. While chromites do maintain their perovskite structure when exposed to the reducing environment on the anode side of an operating SOFC, they experience a loss of lattice oxygen which results in a decrease in electrical conductivity and an increase in volume.[1,2]

The effect of atmosphere on the physical dimensions of doped lanthanum chromites was studied by measuring the linear expansion of sintered specimens as a function of ambient oxygen partial pressure ($P(O_2)$) at several relevant temperatures. After initially equilibrating the specimens in air, the $P(O_2)$ was decreased stepwise using a CO_2/Ar-4% H_2 buffered gas system. The compositions studied were $La_{0.85}Ca_{0.15}CrO_3$ (referenced hereafter as LCC-15), $La_{0.80}Ca_{0.20}CrO_3$ (LCC-20), $La_{0.75}Ca_{0.25}CrO_3$ (LCC-25), and $La_{0.70}Ca_{0.30}CrO_3$ (LCC-30). Figures 1 and 2 show linear expansion as a function of $P(O_2)$ at three temperatures for LCC-20 and LCC-30, respectively. As the $P(O_2)$ was decreased, the physical dimensions of the sintered specimens remained essentially constant until a critical $P(O_2)$ was reached, after which the specimens expanded with decreasing $P(O_2)$. Increases in temperature caused the onset of expansion to occur at higher values of $P(O_2)$. Also, the magnitude of the linear expansion at a

given $P(O_2)$ increased with increasing temperature. Similar behavior was observed for LCC-15 and LCC-25.

Figure 3 shows linear expansion at 1000°C for all four compositions. Increasing Ca content caused the onset of expansion to occur at higher $P(O_2)$ and, for a given value of $P(O_2)$, resulted in an increase in expansion. At 10^{-18} atm $P(O_2)$, linear expansion ranged from 0.12% for LCC-15 to 0.37% for LCC-30. This decrease in stability with increasing Ca content suggests that, for interconnect applications, Ca doping of lanthanum chromite should be no greater than is necessary in order to obtain adequate sinterability and electrical conductivity.

The observed expansion can be correlated to the formation of oxygen vacancies as reported by Anderson.[1,2] A likely explanation lies in the fact that the removal of oxygen anions from the perovskite lattice eliminates the electrostatic attraction between those anions and the surrounding cations and causes increased electrostatic repulsion between those unshielded cations. The net result is an increase in lattice cell dimensions, and, therefore, an increase in specimen volume.

Microstructures of sintered LCC specimens were examined by SEM after exposure to oxidizing environments (control), reducing environments, or sequential exposure to reducing and oxidizing conditions. Control specimens (annealed in air at 1000°C) exhibited no discernible phase segregation or impurity phases at the grain boundaries. Similarly, specimens exposed to a highly reducing atmosphere (10^{-18} atm $P(O_2)$ at 1000°C) showed no discernible phase segregation. However, the highest doped chromite, LCC-30, did exhibit a change in the fracture mechanism. Prior to reduction, fracture was intergranular in nature, whereas in reduced specimens an intragranular fracture mechanism was observed, suggesting that the grains were weakened as a result of the substantial oxygen deficiency and lattice expansion that these samples experienced.

Other microstructural features were noted in the specimens which experienced sequential exposure to reducing and oxidizing environments. In particular, in LCC-30 (after reduction and re-

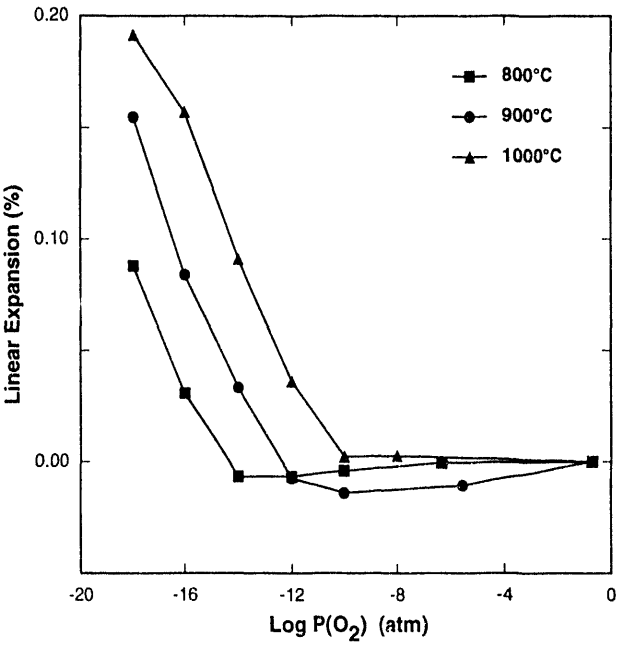

Fig. 1. Linear Expansion vs. Log $P(O_2)$ for LCC-20 at the Indicated Temperatures

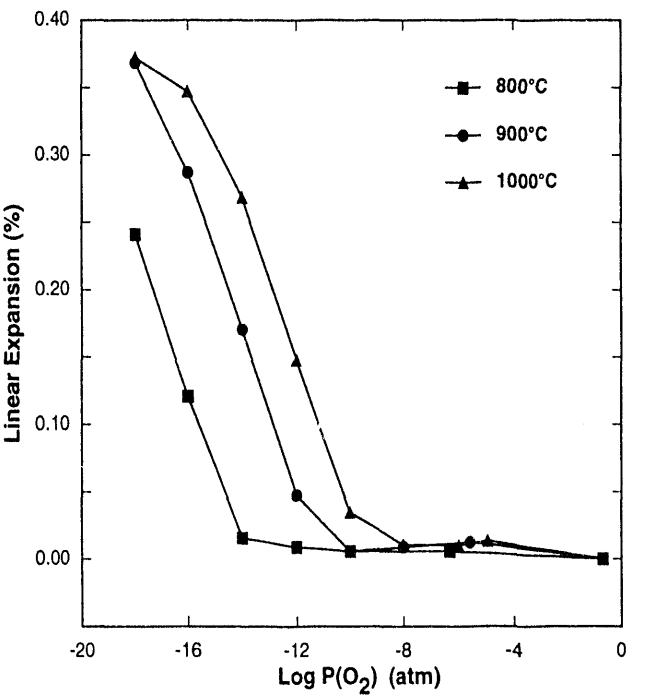

Fig. 2. Linear Expansion vs. Log $P(O_2)$ for LCC-30 at the Indicated Temperatures

oxidation at 1000°C) a Ca and Cr enriched second phase (possibly calcium chromate or an amorphous phase of similar composition) was apparent. Also, while the fracture mechanism after reduction was found to be intragranular in nature, upon re-oxidation the mechanism was intergranular, probably due to the presence of a weak interfacial phase (i.e., calcium chromate or an amorphous phase) at the grain boundaries.

Further evidence for the presence of calcium chromate was found by thermogravimetric analysis of LCC-30 during oxidation-reduction cycles. As expected, a weight loss was measured during reduction due to the removal of lattice oxygen. Upon re-oxidation, a temporary net weight gain occurred in which the specimen weight exceeded its original oxidized weight. With further annealing at temperature in air, the specimen weight decreased to its original value. This net weight gain is consistent with the formation of calcium chromate, in which the Cr cations are oxidized to the +6 valence state. The disappearance of the weight gain with time may result from the decomposition of the calcium chromate phase as the Ca and Cr ions are re-incorporated into the primary perovskite structure, during which process the hexavalent Cr ions would be reduced to the tri- and/or tetravalent state.

Sintering of Doped Lanthanum Manganite

SOFC cathodes must endure severe environmental conditions during operation. For example, the cathode material must be stable at 1000°C in air with high electronic conductivity and a thermal expansion compatible with the YSZ electrolyte. Chemical interaction with the electrolyte and interconnect materials must be minimal. Also, the cathode material must have a highly porous microstructure so that molecular oxygen can diffuse through the cathode to the cathode/electrolyte interface. Given these requirements, it is not surprising that the number of likely candidate materials for SOFC cathodes is very limited. The current preferred material for SOFC applications is lanthanum manganite, $LaMnO_3$, doped with an appropriate amount of Ca or Sr. This material offers adequate electrical conductivity, reasonable thermal expansion match to YSZ, and stability in the SOFC cathode operating environment.[2-5]

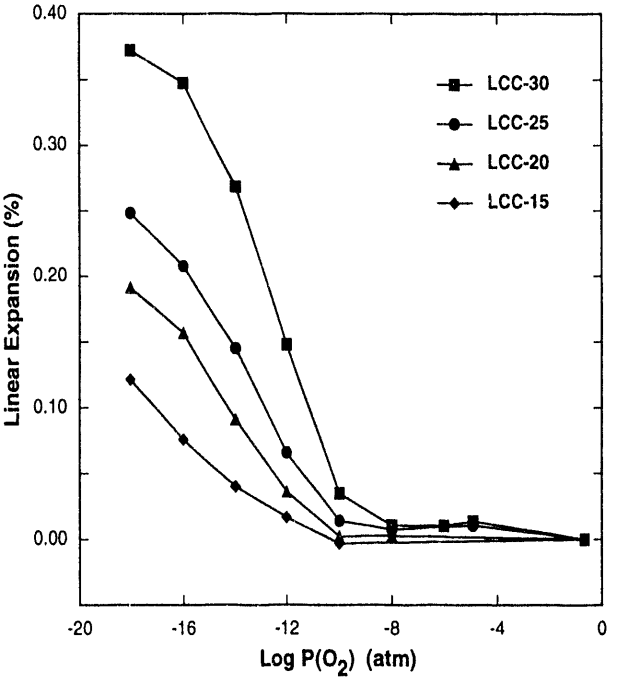

Figure 3. Linear Expansion vs. Log $P(O_2)$ for the Indicated Compositions at 1000°C

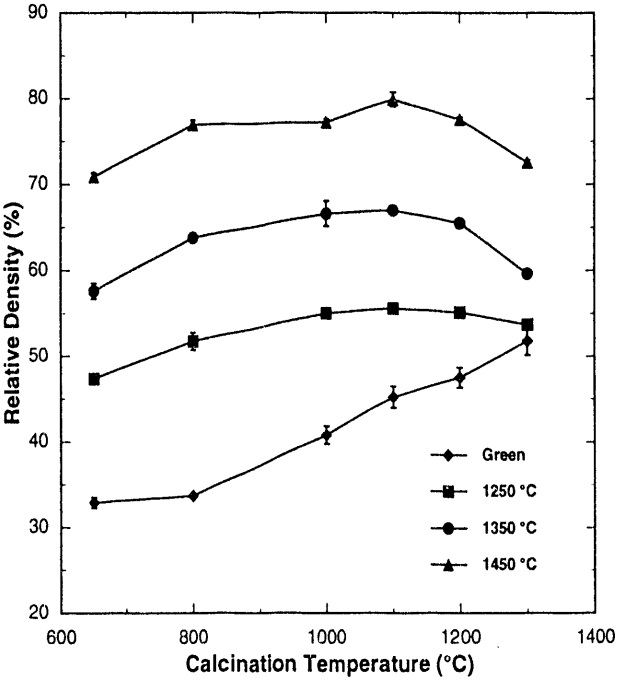

Figure 4. Sintered Density vs. Calcination Temperature for LSM-24

The following compositions were selected for this sintering study due to their close thermal expansion match to YSZ: $(La_{0.84}Sr_{0.16})_xMnO_3$ [referenced hereafter as LSM-16], $(La_{0.76}Sr_{0.24})_xMnO_3$ [LSM-24], $(La_{0.80}Ca_{0.20})_xMnO_3$ [LCM-20], and $(La_{0.70}Ca_{0.30})_xMnO_3$ [LCM-30], with x (i.e., A/B cation ratio) = 0.95, 0.98, 1.00, 1.02, and 1.05. These compositions were synthesized using the glycine-nitrate process,[6] after which they were "pre-calcined" at 650°C for 0.5 hour. The manganite powders were then calcined at a variety of temperatures for 1 hour to determine the effect of calcination temperature on sintering behavior.

The effect of calcination temperature on sintered densities of LSM-24 and LCM-30 (sintered for one hour at the indicated temperatures) is shown in Figures 4 and 5, respectively. Green densities of the dry-pressed compacts are also shown in these figures. The green densities of compacted pre-calcined powders were very low. These low packing densities were caused by extensive particle agglomeration resulting from the synthesis method, which yields nanometer-sized particles which are partially sintered into an open, high surface area network. The pre-calcined manganite powders typically had a bimodal distribution consisting of approx. 15 vol.% 1-2 μm agglomerates and approx. 85% 10-100 μm agglomerates. Coarsening of the powders by calcination reduced the powder surface areas and allowed for improved particle packing densities, so that green density increased with increasing calcination temperature.

Sintered densities were also affected by the calcination temperature. For low calcination temperatures, sintered densities increased with increasing calcination temperature, presumably due to the higher green densities. Sintered densities reached a maximum for powders calcined between 800 and 1200°C, but usually remained below 90% of theoretical due to the agglomerated condition of the powders. For powders calcined above 1200°C, sintered densities tended to decrease substantially, presumably due to the formation of hard agglomerates and the decreasing driving force for densification which occurs with increasing particle size. Figures 4 and 5 also show that, for any given calcination temperature, sintered density increased

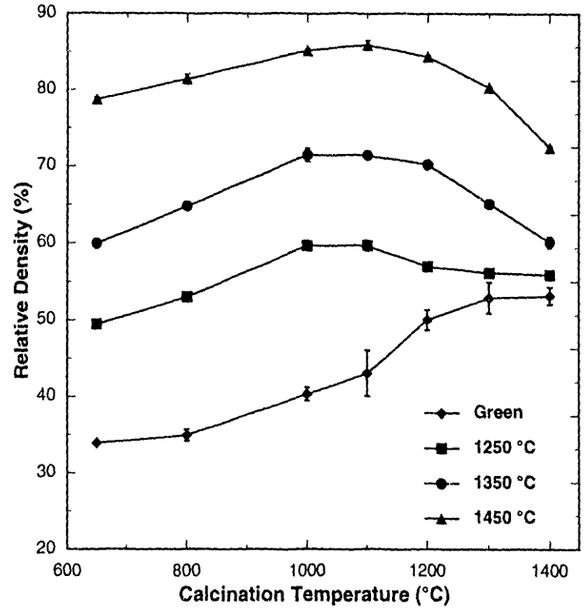

Fig. 5. Sintered Density vs. Calcination Temperature for LCM-30

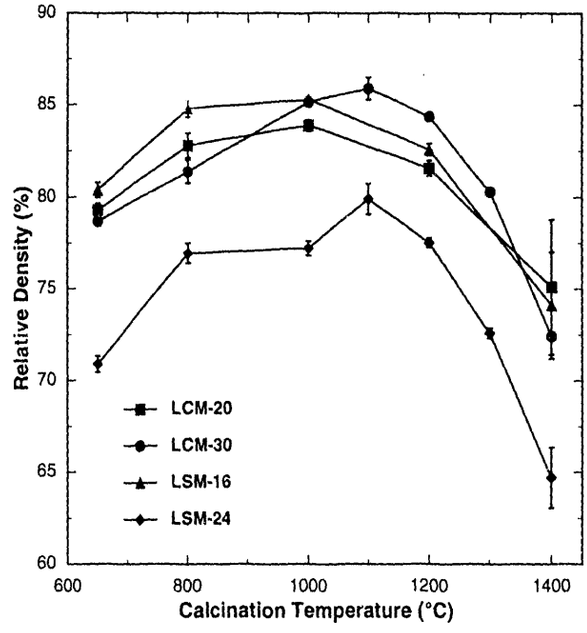

Fig. 6. Sintered Density vs. Calcination Temperature for the Indicated Compositions Sintered at 1450° C

with increasing sintering temperature. Similar results were obtained for LSM-16 and LCM-20. For example, Figure 6 shows the densities for all four lanthanum manganite compositions sintered at 1450°C for 1 hour. With the exception of LSM-24, which exhibited lower densities than the other three compositions, sintered density exhibited little dependence on dopant type and content.

It was found in this study that the sintering behavior of lanthanum manganite is highly dependent on the ratio of A-site cations (La, Sr, Ca) to B-site cations (Mn) present in the material. Compositions were prepared with A/B cation ratios of 0.95, 0.98, 1.00, 1.02, and 1.05. Since it could be safely assumed that all ions present in that structure occupied regular lattice sites,[7] those five ratios would correspond to $(La_{1-y}M'_y)_{0.95}MnO_3$, $(La_{1-y}M'_y)_{0.98}MnO_3$, $(La_{1-y}M'_y)MnO_3$, $(La_{1-y}M'_y)Mn_{0.98}O_3$, and $(La_{1-y}M'_y)Mn_{0.95}O_3$ (M' = Ca or Sr), respectively, in the case of single phase materials. While some of the compositions were indeed determined by XRD analysis to be single phase perovskites, small amounts of additional phases were discovered in others (see below). (For convenience, an oxygen stoichiometry of 3 (rather than $3 \pm \delta$) is assumed, since oxygen nonstoichiometry in highly doped manganites tends to be relatively small).[8]

Figures 7 and 8 show sintered densities for LSM-24 and LCM-30, respectively, as a function of the A/B cation ratio. These figures demonstrate that A-cation deficiency (i.e., A/B ratio < 1) resulted in a significant increase in density. Similar behavior was observed in LSM-16 and LCM-20. This pronounced effect of A/B cation ratio on densification behavior was also observed in shrinkage plots obtained by measuring the linear shrinkage of green compacts as a function of increasing temperature. These plots showed an enhanced shrinkage for A cation deficient manganites relative to stoichiometric and B cation deficient manganites. The shape of these shrinkage plots was consistent with a solid state sintering mechanism; i.e., there were no signs of sudden shrinkage events due to liquid phase formation, as has been reported in lanthanum and yttrium chromites.[9,10]

XRD analysis was performed on specimens

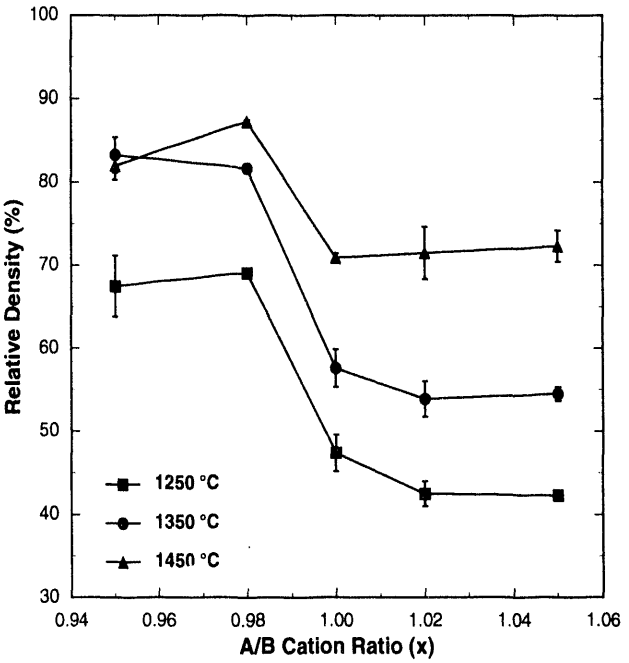

Fig. 7. Sintered Density vs. A/B Cation Ratio for LSM-24

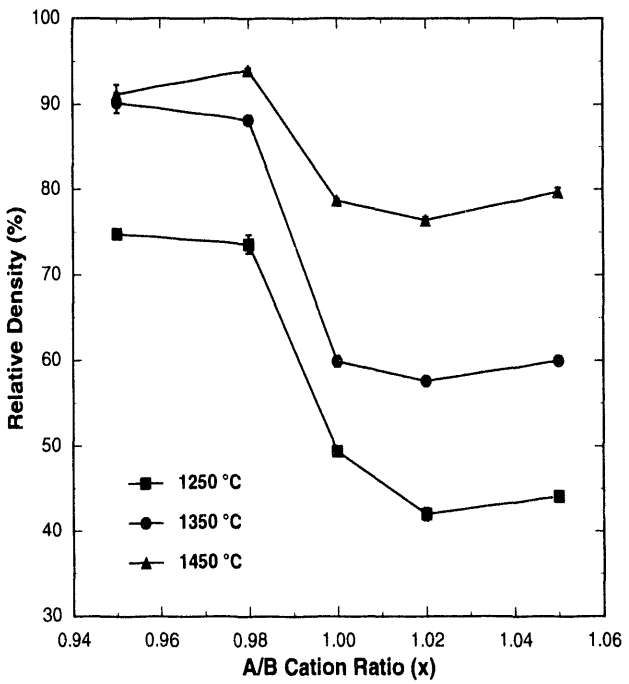

Fig. 8. Sintered Density vs. A/B Cation Ratio for LCM-30

Table I. Minor Phases in Lanthanum Manganite (Approx. Wt.% Shown In Parentheses)

Composition	x=0.95	x=0.98	x=1.00	x=1.02	x=1.05
LSM-16	--	--	--	La_2O_3 (3)	La_2O_3 (5), $La(OH)_3$ (0.5)
LSM-24	Unidentified Spinel (1)	--	--	La_2O_3 (2), $La(OH)_3$ (1)	La_2O_3 (3), $La(OH)_3$ (1)
LCM-20	Mn_3O_4 (0.5)	--	--	--	La_2O_3 (2)
LCM-30	Mn_3O_4 (0.5)	--	--	--	CaO (0.5)

sintered at 1450°C to determine the stability of the perovskite phase as a function of the A/B ratio. The results of this analysis are shown in Table I. La_2O_3 was found in some of the compositions with an A/B ratio greater than 1.00. Since La_2O_3 readily absorbs atmospheric moisture to form $La(OH)_3$ (thereby degrading the strength of the sintered material) it is necessary to avoid the presence of La_2O_3 in lanthanum manganite, so that, overall, an A/B cation ratio in the range 0.98-1.00 appears to be optimal for the synthesis of single phase lanthanum manganites. The addition of pore formers (e.g., organic materials which can be burnt out at low temperatures) may be helpful in obtaining the degree of porosity required for the SOFC cathode application.

In an attempt to find the reason for this difference in sintering behavior, slow XRD scans were performed on LSM-24 powders with A/B ratios of 0.98 and 1.00. This analysis showed that, prior to sintering, both powders consisted primarily of the desired perovskite phase, except for approx. 5 wt.% $SrCO_3$ as a second phase. Also, the surface areas and degree of agglomeration of the manganite powders were determined to be essentially independent of A/B cation ratio.

Since the value of the A/B ratio was the only detectable difference in these powders, the enhanced sinterability of manganites when A/B = 0.98 instead of 1.00 can best be explained by examining the defect chemistry of these materials. Since neither interstitial ions nor wrong site ions are expected to be present in significant numbers,[7] preparation of these materials with A/B < 1.00 should produce an excess concentration of A-site vacancies within the structure. Similarly, manganites with A/B > 1 would have excess B-site vacancies within the structure. The higher densities found in the A cation deficient materials indicate that the diffusion of A-site cations is the limiting factor in the mass transport of ions during densification (as suggested by van Roosmalen et al.[11] for undoped lanthanum manganite). Thus, when excess A-site vacancies are introduced, diffusion of A-site cations occurs more readily, resulting in higher sintered densities. Since the introduction of excess B-site vacancies (A/B > 1.00) had little effect on sintering behavior, the diffusion of B-site cations is apparently not a limiting factor in the densification process.

FUTURE WORK

Future SOFC efforts in FY 1994 will continue to focus on the optimization of state-of-the-art and alternative component materials and fabrication procedures. Specific short-term areas of emphasis include an investigation into the effect of ambient oxygen partial pressure on the stability and mechanical properties of Ca and Sr doped lanthanum chromite and Ca doped yttrium chromite. The viability of composite cathodes will be evaluated by studying the sintering, electrical, and thermal properties of physical mixtures of YSZ and Sr and Ca doped lanthanum manganite. This program will conclude in FY 1994.

REFERENCES

1. H. Anderson, J. Kuo, and D. Sparlin, "Review of Defect Chemistry of $LaMnO_3$ and $LaCrO_3$,"

Proc. 1st Int. Symp. on SOFC, ed. S.C. Singhal, Electrochem. Soc., Proc. Vol. 89-11, 111-128 (1989).

2. S. Srilomsak, D. Schilling, and H. Anderson, "Thermal Expansion Studies on Cathode and Interconnect Oxides," Proc. 1st Int. Symp. on SOFC, ed. S.C. Singhal, Electrochem. Soc., Proc. Vol. 89-11, 129-140 (1989).

3. N.Q. Minh, "Ceramic Fuel Cells," J. Am. Ceram. Soc., **76**, 563-88 (1993).

4. J.H. Kuo, H.U. Anderson, and D.M. Sparlin, "Oxidation-Reduction Behavior of Undoped and Sr-Doped $LaMnO_3$: Nonstoichiometry and Defect Structure," J. Solid State Chem., **83**, 52-60, (1989).

5. J.H. Kuo, H.U. Anderson, and D.M. Sparlin, "Oxidation-Reduction Behavior of Undoped and Sr-Doped $LaMnO_3$: Defect Structure, Electrical Conductivity, and Thermoelectric Power," J. Solid State Chem., **87**, 55-63, (1990).

6. L.A. Chick, L.R. Pederson, G.D. Maupin, J.L. Bates, L.E. Thomas, and G.J. Exarhos, "Glycine-Nitrate Combustion Synthesis of Oxide Ceramic Powders," Materials Letters, **10**, 6-12 (1990).

7. B.C. Tofield and W.R. Scott, "Oxidative Nonstoichiometry in Perovskites, an Experimental Survey; the Defect Structure of an Oxidized Lanthanum Manganite by Powder Neutron Diffraction," J. Solid State Chem., **10**, 183-194 (1974).

8. J.W. Stevenson, M.M. Nasrallah, H.U. Anderson, and D.M. Sparlin, "Defect Structure of $Y_{1-y}Ca_yMnO_3$ and $La_{1-y}Ca_yMnO_3$ I. Electrical Properties, II. Oxidation-Reduction Behavior" J. Solid State Chem., **102**, 175-197 (1993).

9. L.A. Chick, T.R. Armstrong, D.E. McCready, G.W. Coffey, G.D. Maupin, and J.L. Bates, "Low-Temperature Sintering and Phase Changes in Chromite Interconnect Materials," Proc. 3rd Intl. Symp. on SOFC, Ed. S. Singhal and H. Iwahara, Electrochem. Soc., Proc. Vol. 93-4, 374-384 (1993).

10. N. Sakai, T. Kawada, H. Yokokawa, M. Dokiya, and I. Kojima, "Liquid-Phase-Assisted Sintering of Calcium-Doped Lanthanum Chromites," J. Am. Ceram. Soc., **76**, 609-616 (1993).

11. J.A.M. van Roosmalen, E.H.P Cordfunke, and J.P.P. Huijsmans, "Sinter Behaviour of $(La,Sr)MnO_3$," Solid State Ionics, **66**, 285-293 (1993).

Proc. 1st Int. Symp. on SOFC, ed. S.C. Singhal, Electrochem. Soc., Proc. Vol. 89-11, 111-128 (1989).

2. S. Srilomsak, D. Schilling, and H. Anderson, "Thermal Expansion Studies on Cathode and Interconnect Oxides," Proc. 1st Int. Symp. on SOFC, ed. S.C. Singhal, Electrochem. Soc., Proc. Vol. 89-11, 129-140 (1989).

3. N.Q. Minh, "Ceramic Fuel Cells," J. Am. Ceram. Soc., **76**, 563-88 (1993).

4. J.H. Kuo, H.U. Anderson, and D.M. Sparlin, "Oxidation-Reduction Behavior of Undoped and Sr-Doped $LaMnO_3$: Nonstoichiometry and Defect Structure," J. Solid State Chem., **83**, 52-60, (1989).

5. J.H. Kuo, H.U. Anderson, and D.M. Sparlin, "Oxidation-Reduction Behavior of Undoped and Sr-Doped $LaMnO_3$: Defect Structure, Electrical Conductivity, and Thermoelectric Power," J. Solid State Chem., **87**, 55-63, (1990).

6. L.A. Chick, L.R. Pederson, G.D. Maupin, J.L. Bates, L.E. Thomas, and G.J. Exarhos, "Glycine-Nitrate Combustion Synthesis of Oxide Ceramic Powders," Materials Letters, **10**, 6-12 (1990).

7. B.C. Tofield and W.R. Scott, "Oxidative Nonstoichiometry in Perovskites, an Experimental Survey; the Defect Structure of an Oxidized Lanthanum Manganite by Powder Neutron Diffraction," J. Solid State Chem., **10**, 183-194 (1974).

8. J.W. Stevenson, M.M. Nasrallah, H.U. Anderson, and D.M. Sparlin, "Defect Structure of $Y_{1-y}Ca_yMnO_3$ and $La_{1-y}Ca_yMnO_3$ I. Electrical Properties, II. Oxidation-Reduction Behavior" J. Solid State Chem., **102**, 175-197 (1993).

9. L.A. Chick, T.R. Armstrong, D.E. McCready, G.W. Coffey, G.D. Maupin, and J.L. Bates, "Low-Temperature Sintering and Phase Changes in Chromite Interconnect Materials," Proc. 3rd Intl. Symp. on SOFC, Ed. S. Singhal and H. Iwahara, Electrochem. Soc., Proc. Vol. 93-4, 374-384 (1993).

10. N. Sakai, T. Kawada, H. Yokokawa, M. Dokiya, and I. Kojima, "Liquid-Phase-Assisted Sintering of Calcium-Doped Lanthanum Chromites," J. Am. Ceram. Soc., **76**, 609-616 (1993).

11. J.A.M. van Roosmalen, E.H.P Cordfunke, and J.P.P. Huijsmans, "Sinter Behaviour of $(La,Sr)MnO_3$," Solid State Ionics, **66**, 285-293 (1993).

DATE
FILMED
10/17/94

END